Where is the surface-layer turbulence?

Andrei Tokovinin

Cerro Tololo Inter-American Observatory, Casilla 603, La Serena, Chile

ABSTRACT

Remote turbulence sensing in the first 100m above ground using lunar scintillation has revealed that the seeing measured by regular site monitors can be over-estimated. This explains the well-known discrepancy between the VLT image quality and the seeing measured by the DIMM at Paranal. The concept of "site seeing" needs to be critically reviewed, considering strong dependence of this parameter on the height of site monitors and on the local turbulence in their immediate vicinity. Higher resolution of ground-based telescopes can be reached if we accept that the natural seeing can be better than shown by the DIMMs and that the contribution of telescope and its environment to the seeing can be significant on nights with superb conditions. This is particularly relevant to the wide-angle optical and IR telescopes which do not rely on adaptive optics. Eventually, a wide-angle adaptive optics will remove local and instrumental distortions and will deliver images truly limited by the atmosphere.

Keywords: Site testing

1. INTRODUCTION

Optical turbulence is a major factor for ground-based telescopes and interferometers. Background-limited sensitivity to point sources is proportional to D/ε, so a gain of two times in the seeing resolution ε is equivalent to doubling the telescope diameter D. Confusion-limited sensitivity and information content in sky images have an even stronger dependence on ε. Thus, even a small gain in the delivered image quality (DIQ) is worth the effort. Adaptive optics (AO) improves the resolution over narrow fields, but its capabilities also critically depend on the optical turbulence profile (OTP). On the other hand, wide-angle telescopes remain seeing-limited, so far.

Considerable improvement of ground-based resolution has been achieved over past decades by (i) installing telescopes at the best sites, (ii) eliminating or reducing man-made turbulence inside domes and (iii) active correction of aberrations. Measurements of the OTP play a key role in this quest for resolution. Comparison between DIMM seeing and telescope image size served as a guideline to improve optics and local environment, up to the point when telescopes started doing better than predicted by DIMMs.[7,16] It appears, however, that the ultimate resolution is not reached yet; we try to demonstrate below that further progress is possible.

Various instruments exist to measure the OTP. A classical Differential Image Motion Monitor (DIMM)[15] has been recently complemented by profilers based on single-star scintillation (MASS)[9] or wave-front slopes (SLODAR).[13,23] Special effort is devoted to measuring the lowest, most intense turbulent layers with fine vertical resolution. Such data are needed for selecting optimum height of telescope enclosures, for understanding the difference between DIMM seeing and telescope resolution, and for predicting the performance of ground-layer AO, GLAO. Development of future AO instruments is prone to errors if not based on good OTP measurements, as happened in the case of ALTAIR on Gemini-North.[3]

The definition of the OTP and all methods of its measurement are rooted in the Kolmogorov turbulence model or its extensions, where the intensity of optical turbulence is characterized by a single number, refractive-index structure constant C_n^2. The underlying concept of a random stationary process is only a more or less successful approximation to real optical distortions. Atmospheric optical path is usually subdivided into *free atmosphere* (FA), *ground layer* (GL), also called *boundary layer* (BL), and it lower part, *surface layer* (SL). These definitions and height boundaries vary between different authors. Here we concentrate on the SL turbulence, up to few hundred meters above ground.

In this paper, we describe the new technique of SL profiling with lunar scintillation, focusing on its potential caveats. Representative results of SL profiling at three sites are given, showing typical $C_n^2(h)$ dependence and the general weakness of SL turbulence. We propose then to take the existing standard seeing measurements in a new perspective which opens ways for improving telescope performance.

E-mail: atokovinin@ctio.noao.edu

2. SURFACE-LAYER PROFILING WITH LUNAR SCINTILLOMETERS

Figure 1. LuSci installation at Peñon in October 2009. Photo credit: E. Bustos.

Scintillation of stars originates mostly in high atmospheric layers. In contrast, scintillation of extended sources such as Sun or Moon is dominated by turbulence in the SL. This fact, recognized by Codona[5] and Beckers,[2] lead to the development of remote SL profilers for day-time and night-time[8,17] astronomy. A simple lunar scintillometer, Lusci, has been used recently at several sites. This technique has obvious advantages over traditional in-situ measurements with masts. Scintillation is a direct *optical* effect, unlike micro-thermal or acoustic devices which sense the air temperature. Moreover, LuSci is non-destructive, whereas masts, towers, and enclosures can perturb the air flow. Non-destructive turbulence profiling with acoustic sounders, SODARS, is a good alternative, although converting the sonic echo into C_n^2 meets with several problems.[22]

The LuSci instrument[17] consists of 6 photo-diodes of 1-cm diameter placed in a linear non-redundant configuration. Relative flux fluctuations caused by the turbulence can be as small as $\Delta I/I \sim 10^{-4}$; they are recorded with 2-ms sampling and sufficient signal-to-noise ratio. Covariances of the scintillation signals between detector pairs are averaged in time and fitted to a model of a smooth $C_n^2(h)$ profile with few parameters. Lunar phases and instrumental properties (baselines, their orientation, detector size, amplification coefficients) are included in the model. Residuals between the measured covariances and the fitted model are typically within 2% of the scintillation variance.

LuSci data show that turbulence in the SL can be unexpectedly weak – much weaker than inferred from the difference of turbulence integrals measured by DIMM and MASS. This discrepancy is further discussed in the

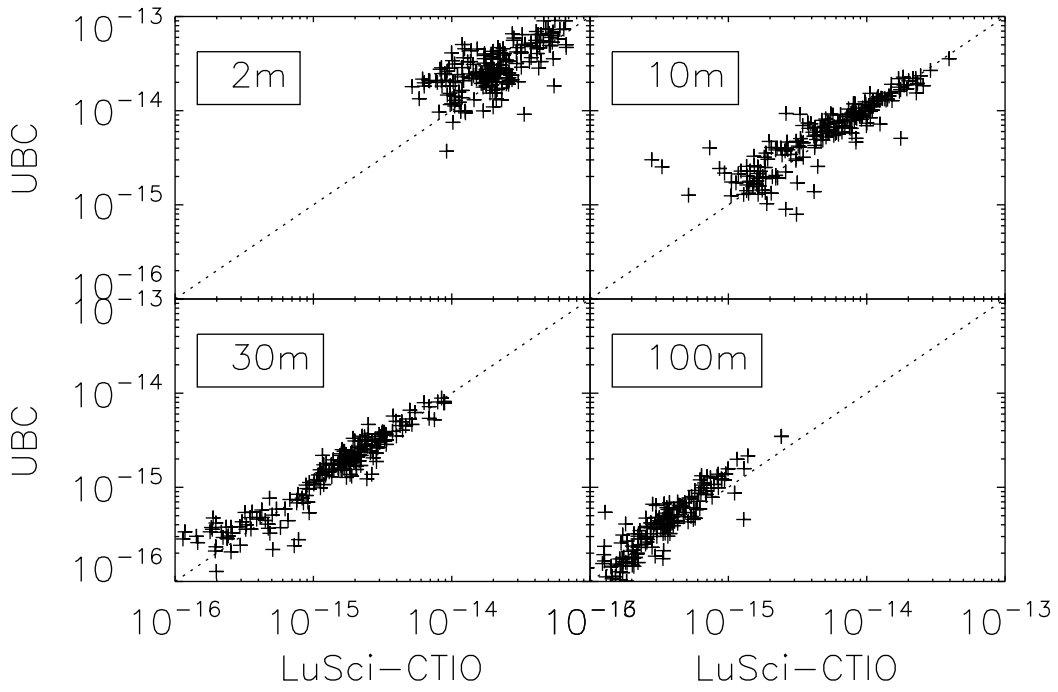

Figure 2. Comparison between C_n^2 at 4 selected heights measured by the UBC scintillometer (vertical axis) and CTIO LuSci (horizontal axis) arrays. Simultaneous data averaged over 5-min. time intervals are plotted. Data from Cerro Tololo, March 2009, 4 nights.

next Sections. Here we review various factors that could cause large systemic errors in LuSci data and show that these data can be trusted. This complements the discussion in Sect. 3.4 of Ref. 17.

Instrumental effects can be numerous and potentially damaging, considering the smallness of the flux fluctuations (amplifier noise, pickup noise, insufficient bandwidth, poor calibration, stray light, etc.). All these factors are carefully controlled in the instrument design. The best proof, however, is offered by comparing two different scintillometers. In March 2009, a 12-channel lunar scintillometer array built at the University of British Columbia (UBC)[8] worked together with two LuSci instruments (one built at CTIO, another at ESO) at Cerro Tololo. The LuSci arrays were operated by A. Berdja and E. Bustos. The remotely-operated UBC scintillometer has smaller 5-mm detectors, different electronics for signal acquisition, different orientation and geometry of the baseline. The covariances measured by the UBC array were kindly provided to us by P. Hickson and used to fit the OTP model in the same way as in LuSci, albeit with a much larger number of baselines. The results of the instrument comparison involving 4 nights of data are plotted in Fig. 2. No systematic bias between the instruments is apparent. The random scatter in this log-log plot is about 0.3 (rms). An even better agreement was found between the two similar LuSci instruments. After all, measurement of relative flux fluctuations is straightforward, and instrument comparison confirms that it is done correctly.

The OTP model fitted to the data consists of power-law segments between 5 points at fixed distances from the instrument (from 3 m to 762 m), with constant C_n^2 values below and above this range. Obviously, an OTP with sharp details (a spike or an abrupt step) will be poorly approximated by a smooth model. However, our study has shown than even in such unfavorable cases the total turbulent energy and its localization are reproduced correctly. The theory of random stationary processes which underlines the definition of C_n^2 allows only for a slow, smooth spatial variation of this parameter. In this context, the vertical resolution of a $C_n^2(h)$ profiler in the SL simply cannot be too high, so a smooth model is adequate.

The weighting functions relating covariances to $C_n^2(h)$ are computed by using the Kolmogorov turbulence model, lunar images at different phases, and detector geometry. Signal averaging during 2-ms sampling time can be also accounted for, but it turns to be of some effect only at heights below $\sim$10 m under strong ground

wind. Scintillation is essentially produced in the geometric-optics regime, by pure wave-front curvature; it is achromatic and does not saturate. LuSci is sensitive to refractive-index fluctuations with spatial scales from 0.01 m to 1 m. The validity of the Kolmogorov spectrum at these scale is generally of little doubt. Other site-testing instruments like DIMM, MASS, or SLODAR, sense perturbations of commensurable scales and would be also affected by a non-Kolmogorov turbulence; moreover, the interpretation of their data in terms of C_n^2 would become questionable. This said, the statistics of refractive-index fluctuations in the SL can deviate from the classical Kolmogorov paradigm because of the vertical-horizontal anisotropy or because of additional optical effects, e.g. produced by the gravity waves.

3. RESULTS OF SL PROFILING

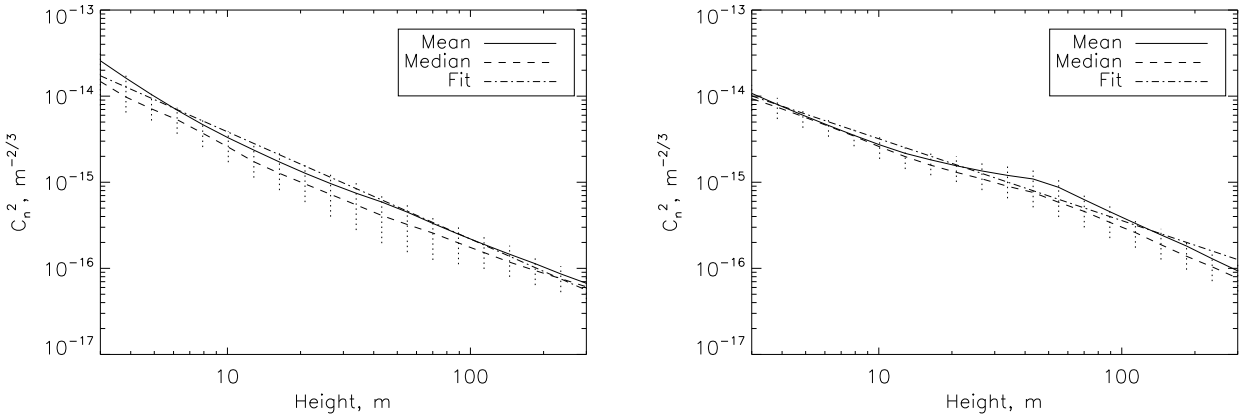

Figure 3. Nightly average OTPs for Nov. 30, 2009 (left) and Dec 1, 2009 (right) at Cerro Peñon. The average OTPs are plotted as full lines, power-law fits as dash-dotted lines. The dashed lines with dotted vertical segments indicate median values, 25% and 75% quartiles of C_n^2 at each height.

Lunar scintillometers have been operated over past few years at several observatories in Chile. At each site, the intensity of turbulence in the SL and its vertical profile are highly variable. Nevertheless, some common trends emerge. The discussion below is focused on three sites: Cerro Paranal hosting the Very Large Telescope (VLT), Cerro Pachón with Gemini-South and SOAR telescopes (and its peak Peñon reserved for the LSST), and the Cerro Tololo observatory. We also invoke the Mauna Kea observatory.

The OTP shape is typically close to a power law, showing a steep decrease of $C_n^2(h)$ with the height h above the ground. An example is given in Fig. 3 for Cerro Peñon, where about 200 profiles per night were recorded around full Moon in November-December 2009. The Figure plots nightly average and median C_n^2 values versus height. On these two nights, the OTPs were only moderately variable, so averages and medians are close to each other. The logarithms of the average OTPs were fitted by straight lines

$$\log_{10} C_n^2(h) \approx A + p \log_{10}(h/1\mathrm{m}) \tag{1}$$

in the range $3 < h < 300$ (h in meters, C_n^2 in m$^{-2/3}$). For the two nights shown in Fig. 3, $A = (-13.17, -13.54)$, $p = (-1.24, -0.95)$. For the totality of the data obtained in this full-Moon period (12 nights, 1861 profiles), $A = -13.38$ and $p = -1.16$. Similar fits characterize the data obtained at Cerro Paranal and Cerro Tololo (Fig. 4). Despite strong variability of both individual OTPs and their nightly averages, these power-law fits show the general trend.

The power-law model is different from the negative-exponential law proposed in Ref. 21 for Cerro Pachón, although both models coincide in the range $h = (10, 30)$ m, predicting $C_n^2 \sim 10^{-15}$ m$^{-2/3}$ at $h = 30$ m. Unlike the exponential model, the integral of the power-law from 0 to ∞ is infinite, making it difficult to define the SL seeing in a consistent way.

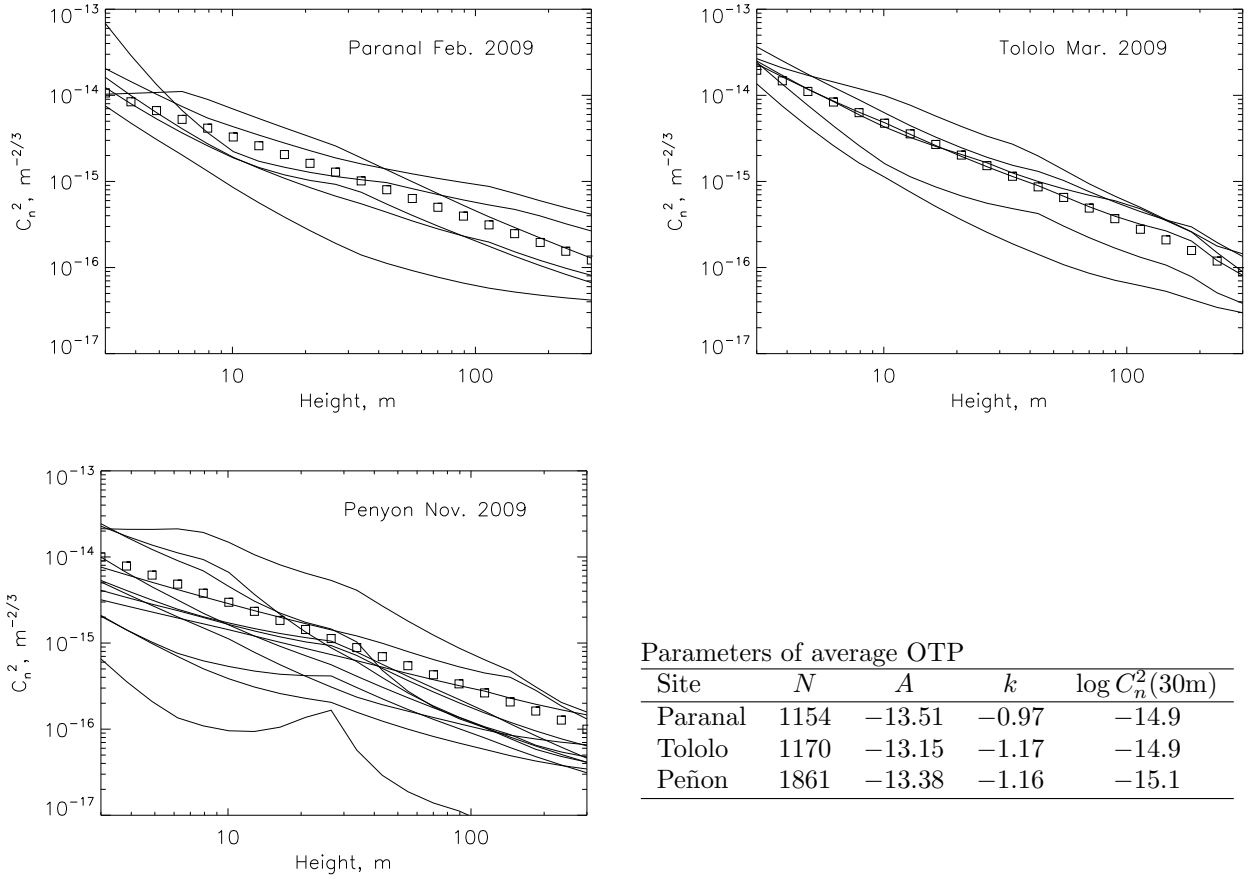

Parameters of average OTP

Site	N	A	k	$\log C_n^2(30\mathrm{m})$
Paranal	1154	−13.51	−0.97	−14.9
Tololo	1170	−13.15	−1.17	−14.9
Peñon	1861	−13.38	−1.16	−15.1

Figure 4. Nightly average OTPs at three sites (lines) and power-law models (squares). The total number of individual OTPs N and the parameters of the power-law fits (1) are listed in the table.

The SL seeing $\varepsilon_{\rm SL}$ is determined by the turbulence integral $J_{\rm SL}$, $\varepsilon_{\rm SL} = (J_{\rm SL}/6.8 \times 10^{-13})^{0.6}$ acrseconds, where

$$J_{\rm SL} = \int_{h_{\rm min}}^{h_{\rm max}} C_n^2(h)\mathrm{d}h \tag{2}$$

and the limits $(h_{\rm min}, h_{\rm max})$ set the SL boundaries. For a meaningful comparison with DIMM and MASS, the lower limit coincides with the DIMM height above ground (6 m), the upper limit is set at 500 m. As the MASS sensitivity to turbulence increases smoothly towards 500 m, we account for this weighting in the calculation of the SL integrals from the LuSci data. Considering the typical weakness of turbulence in the 250–500 m range, the choice of $h_{\rm max}$ and this weighting have little effect on the calculated $J_{\rm SL}$, which are dominated by the contribution from the lower heights.

The power-law OTP (1) leads to turbulence integrals (in $\mathrm{m}^{1/3}$):

$$J_{\rm SL} = 10^A/(k+1)\ [h_{\rm max}^{k+1} - h_{\rm min}^{k+1}],\ \ k \neq -1 \tag{3}$$

$$J_{\rm SL} = 10^A\ \ln(h_{\rm max}/h_{\rm min}),\ \ k = -1. \tag{4}$$

The fits for Paranal, Tololo, and Peñon presented in Fig. 4 correspond to the $J_{\rm SL}$ integrals from 6 m to 500 m of 1.54, 1.62, and 0.99 in units of $10^{-13}\,\mathrm{m}^{1/3}$, or the SL seeing of 0.41″, 0.42″, and 0.31″, respectively. As these integrals are derived from the *average* OTPs, they over-estimate the actual medians, which are 0.89, 1.15, and $0.55 \times 10^{-13}\,\mathrm{m}^{1/3}$ for the same three data sets. For comparison, the typical SL integral at Cerro Pachón estimated

in Ref. 21 from a variety of data sources is $2.7 \times 10^{-13}\,\mathrm{m}^{1/3}$ and corresponds to the $0.5''$ seeing contribution from the SL.

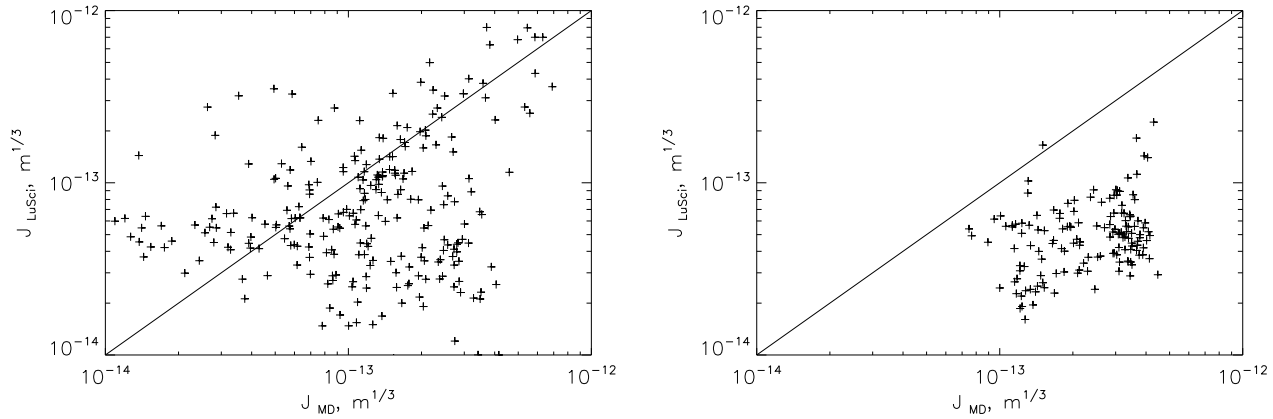

Figure 5. Comparison of SL turbulence integrals measured simultaneously by LuSci (vertical axis) and DIMM minus MASS (horizontal axis). Left: Cerro Peñon, November-December 2009. Right: Cerro Tololo, March 2009 (SL profiles from the UBC array). The straight lines show 1:1 correspondence.

Comparison between J_{LuSci} calculated from LuSci profiles with the estimate of SL turbulence obtained from MASS and DIMM, $J_{\mathrm{MD}} = J_{\mathrm{DIMM}} - J_{\mathrm{MASS}}$, is shown in Fig. 5 for two campaigns. Each point represents a 5-min average over coincident time intervals. At Cerro Peñon, there was no MASS monitor; simultaneous data from the MASS at the nearby Cerro Pachón were used instead, assuming that turbulence in the free atmosphere is same at both locations. We see that most points lie below the diagonals, especially at Cerro Tololo. An even stronger case of disagreement is presented in Fig. 12 of Ref. 17 for Paranal, where the SL integrals measured by LuSci and MASS-DIMM show a good correlation, but differ by almost an order of magnitude; the median values are 3.6×10^{-13} and 0.41×10^{-13} for J_{MD} and J_{LuSci}, respectively. Small values of J_{LuSci} at Paranal are confirmed by simultaneous measurements with SL-SLODAR and by micro-thermal measurements with mast in 1998.[12] Similarly small J_{LuSci} are seen in Fig. 5 (right) at Cerro Tololo.

Considering the robustness of LuSci results against all kinds of systematic effects (see above), their direct and indirect agreement with the OTPs measured by other methods, and good agreement with MASS and DIMM in the case of strong SL turbulence at Cerro Peñon, the discrepancy between J_{LuSci} and J_{MD} must be real (i.e. not an instrumental effect). We discuss this *SL discrepancy* below.

4. REASONS OF THE SL DISCREPANCY

4.1 Data compilation

Available data show that turbulence in the SL is usually weak, $C_n^2 \sim 10^{-15}\,\mathrm{m}^{-2/3}$ at $h = 30\,\mathrm{m}$. Considering typical values $J_{\mathrm{SL}} \sim 3 \times 10^{-13}\,\mathrm{m}^{1/3}$ measured with DIMM and MASS at Paranal and other sites, a 300-m layer of turbulence with $C_n^2 \sim 10^{-15}\,\mathrm{m}^{-2/3}$ is implied. Where is this layer?

Table 1 gives a compilation of published and new measurements of median J_{SL} integrals obtained by a variety of techniques at four sites. Data from LuSci are presented twice when they are compared with other instruments on matching time intervals, e.g. 5-min. averages for comparisons with DIMM−MASS or 20-s samples for comparison with SL-SLODAR. One can't help noticing the disparity of values at each site, with larger estimates provided by DIMMs and smaller estimates from optical remote sensing and micro-thermal probes.

One of the first SL studies at Paranal was done in 1998 and revealed weak microthermal turbulence at the elevation of DIMM.[12] This result, in seeming contradiction with current ideas,[11,16] was confirmed independently by a good agreement between the two seeing monitors installed at 3 m and 6 m above ground. This agreement has been interrupted by a strong local turbulence only for a small fraction of time during that 19-night campaign,

Table 1. Median surface-layer turbulence integrals

Site	$(h_{\min}, h_{\max})$ m	$J_{\rm SL}$ $10^{-13}\,{\rm m}^{1/3}$	N	Method	Period, Reference
Paranal	3, 21	0.40	9 nights	mast	Nov-Dec 1998[12]
Paranal	6, 500	0.41	110, 5-min	LuSci	Feb. 2009[17]
Paranal	6, 500	3.60	110, 5-min	DIMM−MASS	Feb. 2009[17]
Paranal	6, 65	0.47	2096	LuSci	Feb. & Apr. 2009[17]
Paranal	6, 65	0.64	2096	SL-SLODAR	Feb. & Apr. 2009[13,17]
Paranal	3, 100	2.66	70 nights	SLODAR	Feb 2005 - Jan 2006[23]
Pachón	6, 700	1.14	43	Balloon	1998[1]
Pachón	6, 500	2.37	6619	DIMM−MASS	2005[21]
Peñon	6, 500	0.55	1861	LuSci	Nov-Dec 2009
Peñon	6, 500	1.06	329, 5-min	LuSci	Nov-Dec 2009
Peñon	6, 500	1.16	329, 5-min	DIMM−MASS	Nov-Dec 2009
Tololo	6:, 500	1.80	6900	SCIDAR	1998[1]
Tololo	6, 500	3.40	22300	DIMM−MASS	2003[18]
Tololo	6, 500	2.88	43316	DIMM−MASS	Apr 2004 - Dec 2008[6]
Tololo	6, 500	1.15	1170	UBC array	March 2009
Tololo	6, 500	0.49	145, 5-min	UBC array	March 2009
Tololo	6, 500	2.53	145, 5-min	DIMM−MASS	March 2009
Mauna Kea	13, 700	0.86	6530	SCIDAR	Oct 2002[20]
Mauna Kea	13, 500	1.73	924	DIMM−MASS	Oct 2002[20]
Mauna Kea	13, 93	1.72	27198	SLODAR	Oct. 2006 - Jul 2008[4]
Mauna Kea	13, 28	1.90	1104	LOLAS	Oct. 2007 - Jul 2008[4]
All	6, 100:	0.45	-	seeing model	Racine[14]

with the median seeing of 0.88″ and 0.87″ at 3 m and 6 m, respectively. On several nights, the DIMM at 6 m measured an even larger seeing than the GSM at 3 m.

Interestingly, SLODARs at Paranal and Mauna Kea measured $J_{\rm SL}$ in excellent agreement with DIMM−MASS. However, these integrals are dominated by the first resolution bin. Once this bin is ignored and SLODAR is used only as a *remote* turbulence sensor, it measures small turbulence integrals in good agreement with LuSci.[11,17] This suggests that optical turbulence is generated in the immediate vicinity of a site-testing instrument, being much weaker in the free air at the same elevation. Osborn et al.[13] compared turbulence integrals from 6 m up derived from the SL-SLODAR in the remote-sensing mode (excluding the lowest bin) with the same integrals measured by the DIMM and found that under excellent seeing DIMM measures larger turbulence, whereas under average and bad seeing the two instruments agree very well (their Fig. 7).

High-resolution turbulence profiling at Mauna Kea[4] establishes the scale height of the SL turbulence *measured from the roof of 2.2-m telescope building* at $\sim$ 28 m, with a large uncertainty about local effects caused by the building. Apparently, at Mauna Kea, as at Paranal, substantial contribution to $J_{\rm SL}$ arises from the local turbulence.

Racine[14] proposes a model where the seeing depends only on altitude of the observatory and on the elevation of the instrument. According to this model, the SL scale height is 2 m and the SL integral is only $0.45\times10^{-13}\,{\rm m}^{1/3}$ at elevation 6 m and at altitude 2400 m. This is only a small contribution to the total seeing produced by the BL and FA. It follows from his Table 1 that seeing measured at Paranal is 0.16″ worse than predicted by the model, implying an additional contribution of $2\times10^{-13}\,{\rm m}^{1/3}$ to the total integral. This is similar to the differences between intrusive and non-intrusive techniques documented in Table 1.

4.2 Boundary-layer turbulence

The discrepancy between DIMM−MASS and LuSci or SL-SLODAR may arise because MASS instruments underestimate the FA turbulence. Indeed, the uncertainty of turbulence strength in the lowest MASS layer at $h =$ 0.5 km is large, hence even small errors in the calibration parameters or profile restoration can, in principle,

affect this layer substantially or move the effective lower boundary of MASS to a higher elevation, say to 1 km. A turbulence in the "grey zone" at $h = 100...1000$ m would then be the major contributor to the ground-layer seeing.

Substantial turbulence in the lowest MASS layer at 0.5-km is indeed often detected at Cerro Pachón (Fig. 5 in Ref. 21). Despite this, the neighboring Cerro Peñon shows less discrepancy between DIMM−MASS and LuSci (Fig. 5, left) than other sites. On the other hand, turbulence at 0.5-km is very weak at Paranal where the SL discrepancy is large. According to the extensive SLODAR study at Paranal,[23] major contribution to $J_{\rm SL}$ (with $h_{\rm max} = 1$ km) comes from the layers below 50 m, not from the BL (their Fig. 4). They find that MASS can indeed under-estimate turbulence intensity at 0.5-km when it is weak, but gives correct results otherwise. This feature is of no consequence because the grey zone does not dominate the $J_{\rm SL}$.

To eliminate MASS from the equation, we computed the SL integrals at Paranal in February 2009 as a difference between DIMM and SL-SLODAR integrals, the latter corresponding to turbulence above ∼60 m. In 42% of cases this resulted in "negative" $J_{\rm SL}$, the remaining 293 points are still systematically larger than $J_{\rm LuSci}$ by a factor of ∼3 (medians $1.34 \times 10^{-13}\,{\rm m}^{1/3}$ and $0.37 \times 10^{-13}\,{\rm m}^{1/3}$, respectively).

4.3 Local turbulence

We come to the conclusion that turbulence within few meters from the site monitor can make a substantial contribution to the measured seeing and $J_{\rm SL}$. These distortions are generated by the instrument or its tower, while turbulence in the free air at the same elevation is normally much weaker.

Most convincing demonstration of local turbulence in a DIMM is given by Els et al.[6] In the worst case of the 3 m/s Northern wind, the CTIO DIMM over-estimates $J_{\rm SL}$ by a factor of two (their Fig. 5), and these distortions are created within 1 m from the instrument. Final statistics for Cerro Tololo derived in Ref. 6 includes empirical correction for the local turbulence. The TMT site monitor used as a reference had a more open enclosure, so it is plausible that less local turbulence is created around this instrument. However, claiming that these DIMMs are *completely* free from the man-made seeing would be premature without further study.

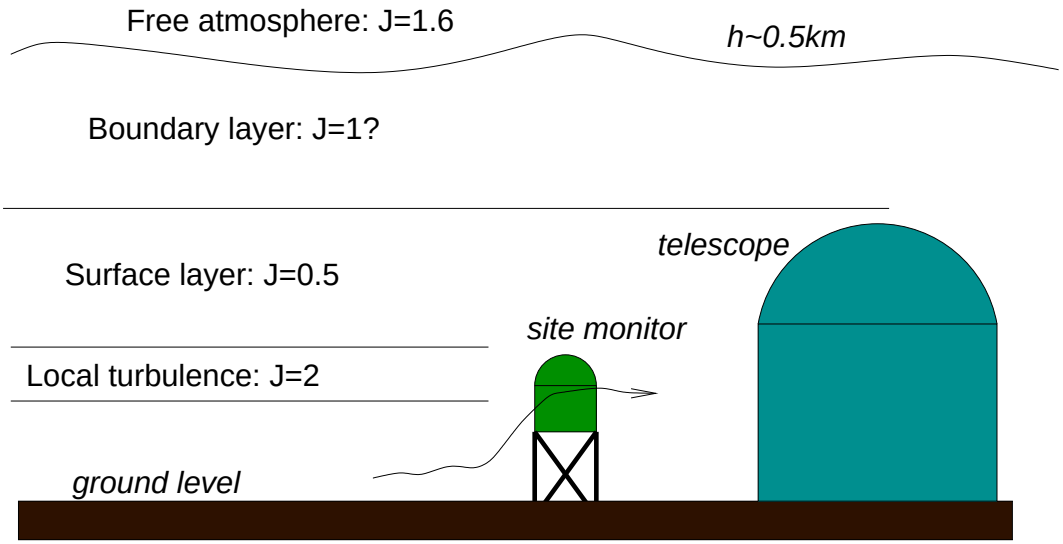

Figure 6. Schematic representation of a good observatory with a sub-division of the light path into zones. Representative values of turbulence integrals J in each zone are given in $10^{-13}{\rm m}^{1/3}$ units and correspond to the seeing of $0.62''$ without local turbulence and $0.84''$ with it.

It is assumed (usually implicitly) that site-testing instruments like DIMM or SLODAR do not cause additional distortions and provide turbulence integral from their elevation upwards. The same assumption is made when the seeing expected in a telescope is calculated as turbulence integral starting from the height of its primary mirror or even from the top of the enclosure. New results obtained with LuSci and re-analysis of the published data challenge this simplistic view. An additional turbulence from local effects, $J_{\rm loc}$, must be considered as a

contribution to the data from seeing monitors. Moreover, turbulence in the SL is not horizontally stratified and is non-homogeneous.

A cartoon in Fig. 6 depicts a typical situation at a good observatory. The values of turbulence integrals are only illustrative. The point is that turbulence in the free air in the vicinity of a site monitor makes only modest contribution to the overall seeing, but the effect of locally generated turbulence near the monitor itself can be substantial. This local turbulence is produced by mixing air with different temperatures – the same phenomenon that creates "regular" turbulence near the ground. The air flow is disturbed by the monitor, creating man-made seeing or, equivalently, reducing the effective elevation of the site monitor. Common origin of local and SL turbulence, as well as extreme variability of both, do not allow their easy separation.

Obviously, telescope enclosures should also create some local optical distortions. However, higher elevation of domes means that temperature gradients in the free air are smaller, while their low-emissivity coatings generate less cold air by contact with the structure.

Locally-generated optical distortions are not expected to follow the Kolmogorov model. Their description by an additive component $J_{\rm loc}$ in the total turbulent integral is thus very crude. As local turbulence depends on many details (temperature gradients, wind direction, construction of the site monitor and its enclosure, and even its color), it can be more or less prominent at various sites and in various conditions. Being negligible under poor seeing, local distortions can dominate under excellent conditions.

4.4 Can a DIMM predict the telescope image quality?

It is well established that the delivered image quality (DIQ) in the VLT telescopes is systematically better than the seeing measured with DIMM.[16] This difference depends on the wind direction and on the temperature gradient in the first 30 m above ground.[11] It was attributed to the strong turbulence in the SL which affects DIMM to a larger extent than the VLT. However, turbulence profiling of the SL at Paranal with LuSci and SL-SLODAR has demonstrated that its intensity is not strong enough to explain this difference without invoking additional contribution from $J_{\rm loc}$.

On the other hand, the DIMM seeing at Las Campanas agrees very well with the DIQ in the Magellan telescope, once the outer-scale effect is accounted for.[7] Of course, the designs of the DIMM tower and Magellan enclosure are different from those at Paranal. Outside air is sucked inside the DIMM tower, otherwise the seeing measurements are degraded (J. Thomas-Osip, private communication). The DIMM at Cerro Tololo is installed in the identical tower as at Las Campanas, but without air sucking; it shows a strong man-made seeing.[6]

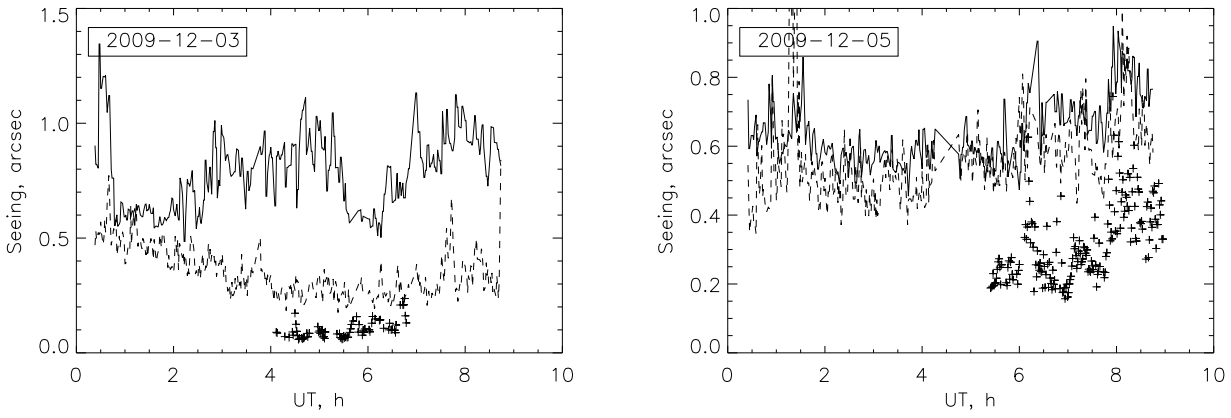

Figure 7. Seeing evolution vs. time for the nights of Dec. 3, 2009 (left) and Dec. 5, 2009 (right) at Cerro Peñon. Full lines – DIMM, dashed lines – MASS, crosses – LuSci.

5. DISCUSSION AND CONCLUSIONS

New results obtained with LuSci challenge standard interpretation of the existing site-testing data by showing that they can be affected by local turbulence in the immediate vicinity of a site monitor. As a consequence, the overall seeing and the intensity of the SL turbulence are over-estimated. This is particularly important at sites with excellent conditions. To illustrate the point, Fig. 7 shows two nights at Cerro Peñon. On the first night with calm FA and exceptionally low SL turbulence, the DIMM seeing still fluctuates between $0.6''$ and $1''$, apparently due to local turbulence. On the second night, the SL is also calm, while the seeing is dominated by a turbulent layer at 1 km and there is no evidence for local turbulence in the DIMM.

Non-intrusive turbulence profiling in the SL has shown, to our surprise, that turbulence in the SL can be very weak, producing at times a seeing of only $0.2''$, instead of $0.5''$ usually assumed. Suppose that on a good night the seeing in the free atmosphere is $0.25''$. The total seeing is then $0.34''$ ($r_0 = 0.3$ m at $0.5\,\mu$m wavelength). Assuming further a typical turbulence outer scale of 25 m, the DIQ in a perfect telescope would be $0.25''$ at $0.5\,\mu$m wavelength and even better in the IR. Reaching such a high resolution without AO correction and in a wide field is a new challenge for the ground-based astronomy.

The quest for higher resolution from the ground is not yet over. Previous round of telescope optimization in the 1990-s (active optics, dome environment) brought telescope DIQ into agreement with the DIMM seeing, or even made it better in the cases of VLT and Magellan. This achievement does not mean, however, that all work on optimization of telescopes and their environment is done. As current DIMMs may be affected by the local turbulence, there is further room for improvement of large telescopes.

Reaching the true atmospheric resolution limit by only passive means may be impractical. When site-testing instruments like SCIDAR or SLODAR work through a telescope, they invariably show a presence of internal seeing. The internal seeing can be reduced, but probably will never be eliminated completely. Taken together with residual static and dynamic aberrations in the optics and vibrations caused by the wind, mount drives, and cryo-coolers, these distortions would require active correction on a relatively rapid time scale. Thus, active optics will eventually evolve towards fast adaptive correction of telescope defects and local turbulence – a wide-field ground-layer adaptive optics (GLAO). A 1-degree GLAO system, IMAKA, is proposed for the 3.6-m CFHT telescope at Mauna Kea[10] as a direct consequence of the site study for Gemini GLAO.[4] In such a wide field, sufficiently bright natural guide stars can be found. Alternatively, future GLAO systems can use cheap low-altitude Rayleigh laser guide stars, as in the SAM instrument.[19]

The second obvious conclusion from this study is that seeing measurements with DIMMs should be taken with caution. The usual assumption that DIMMs are non-intrusive and that the seeing in a large telescope can be predicted from the DIMM data by subtracting the contribution from the intervening layers does not work at Paranal or Cerro Tololo, but seems to work well at Las Campanas. New designs of site monitors and their enclosures may be required to reduce local turbulence to an acceptable level.

Considering strong dependence of SL turbulence on elevation and location, its non-stationary character, and uncontrolled bias in seeing measurements created by local turbulence, the very concept of "site seeing" becomes of questionable value. Measurement of one single parameter, "seeing", should be replaced by monitoring of the OTP. We cannot agree with Racine[14] that site-testing efforts are futile because seeing depends only on altitude and elevation. On the contrary, considerable differences between nearby similar sites, such as Las Campanas and La Silla or Paranal and Armazones, show that further efforts in turbulence characterization are justified. These efforts will be rewarded by increased resolution of existing and future ground-based telescopes.

ACKNOWLEDGMENTS

This work makes a direct or indirect use of data obtained at several observatories by many people. E. Bustos (CTIO) made the most significant contribution to the development and operation of LuSci scintillometers. We want to mention G. Lombardi, A. Berdja, P. Hickson and are particularly thankful to M. Sarazin who enthusiastically supported the fabrication and deployment of lunar scintillometers and made critical and helpful comparisons of their results with other data at Paranal.

REFERENCES

[1] Avila, R., Vernin, J., Chun, M., Sánchez, J.L., "Turbulence and wind profiling with generalized scidar at Cerro Pachón," Proc. SPIE 4007, 721-732 (2000).

[2] Beckers, J. "A Seeing Monitor for Solar and Other Extended Object Observations," Exp. Astr. 12, 1-20 (2001).

[3] Boccas, M., Rigaut, F., Bec, M. et al., "Laser guide star upgrade of Altair at Gemini North," Proc. SPIE, 6272, 114 (2006).

[4] Chun, M. R., Wilson, R., Avila, R. et al., "Mauna Kea ground-layer characterization campaign," MNRAS 394, 1121-1130 (2009).

[5] Codona, J., "The scintillation theory of eclipse shadow bands," Astron. Astrophys. 164, 415-427 (1986).

[6] Els, S.G., Schöck, M., Bustos, E. et al., "Four years of optical turbulence monitoring at the Cerro Tololo Inter-American Observatory (CTIO)," PASP 121, 922-934 (2009).

[7] Floyd, D., Thomas-Osip, J., Prieto, G., "Seeing, wind and outer scale effects on image quality at the Magellan telescopes," Astro-Ph, arXiv1005.0174 (2010).

[8] Hickson, P., Pfrommer, T., Crotts, A., "Optical turbulence profiles at CTIO from a 12-element lunar scintillometer,", In: Optical Turbulence: Astronomy Meets Meteorology, eds. E. Masciadri, M. Sarazin, ESO, 26-33 (2009).

[9] Kornilov, V., Tokovinin, A., Voziakova, O. et al., "MASS: a monitor of the vertical turbulence distribution," Proc. SPIE 4839, 837-845 (2003).

[10] Lai, O., Cuillandre, J.-Ch., Chun, M.R. et al., "Imaka:. Imaging from Mauna Kea", in: Optical Turbulence: Astronomy Meets Meteorology, eds. E. Masciadri, M. Sarazin, ESO, 291-298 (2009).

[11] Lombardi, G., Melnick, J., Hinojosa Goñi, R.H. et al., "Surface layer characterization at Paranal observatory," Proc. SPIE 7333, paper 159 (2010).

[12] Martin, F., Conan, R., Tokovinin, A. et al., "Optical parameters relevant for high angular resolution at Paranal from GSM instrument and surface layer contribution," Astron. Astrophys. Suppl. Ser. 144, 39-44 (2000).

[13] Osborn, J., Wilson, R., Butterley, T. et al., "Profiling the surface layer of optical turbulence with SLODAR," MNRAS, in print (2010).

[14] Racine, R., "Altitude, elevation, and seeing," PASP 117, 401-410 (2005).

[15] Sarazin, M., Roddier, F., "The ESO differential image motion monitor," Astron. Astrophys. 227, 294-300 (1990).

[16] Sarazin, M., Melnick, J., Navarrete, J., Lombardi, G., "Seeing is believing: new facts about the evolution of seeing on Paranal," ESO Messenger 132, 11-17 (2008).

[17] Tokovinin, A., Bustos, E., Berdja, A., "Near-ground turbulence profiles from lunar scintillometer," MNRAS 404, 1186-1196 (2010).

[18] Tokovinin, A., Baumont, S., Vasquez, J., "Statistics of turbulence profile at Cerro Tololo," MNRAS 340, 52-58 (2003).

[19] Tokovinin, A., Thomas, S., Gregory, B. et al., "Design of ground-layer turbulence compensation with a Rayleigh beacon," Proc. SPIE 5490, 870-878 (2004).

[20] Tokovinin, A., Vernin, J., Ziad, A., Chun, M., "Optical turbulence profiles at Mauna Kea measured by MASS and SCIDAR," PASP 117, 395-400 (2005).

[21] Tokovinin, A., Travouillon, T., "Model of optical turbulence profile at Cerro Pachón," MNRAS 365, 1235-1242 (2006).

[22] Travouillon, T., Riddle, R., Skidmore, W., Schöck, M., Els, S., "Correlating Sodar Turbulence Measurements with Ground Heat Flux Data," in: Optical Turbulence: Astronomy Meets Meteorology, eds. E. Masciadri, M. Sarazin, ESO, 248-255 (2009).

[23] Wilson, R.W., Butterley, T., Sarazin, M., "The Durham/ESO SLODAR optical turbulence profiler," MNRAS 399, 2129-2138 (2009).